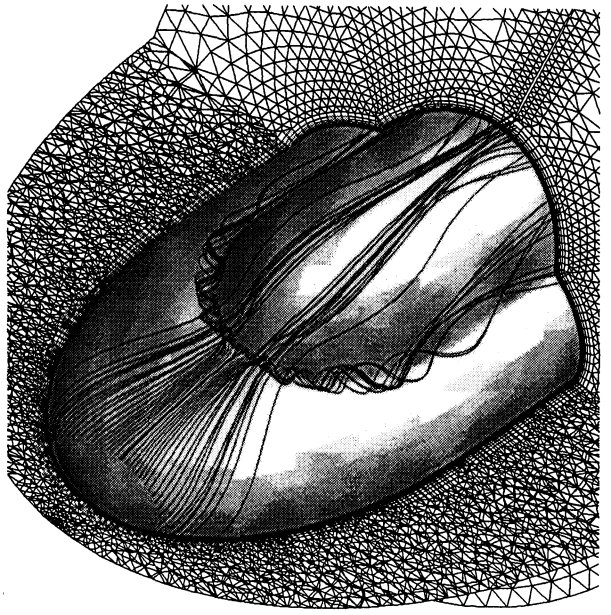

Fig. 3 Double ellipsoid; streamlines and grid.

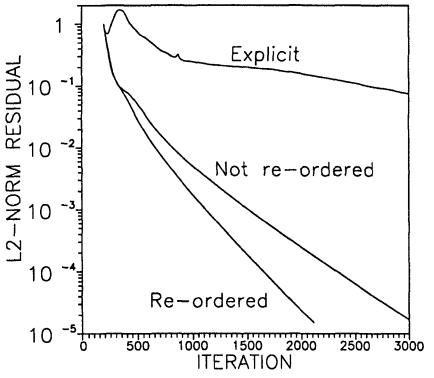

Fig. 4 Convergence history for double ellipsoid.

our experience, the discussed method is unconditionally stable for isotropic grids; however, for highly stretched grids with aspect ratios of order of 1000, the method becomes conditionally stable. It coincides with similar behavior of the structured grid LU-SGS method.

From Fig. 4 we can see that the implicit method converges much faster than the explicit one. For inviscid computations, which are not shown here, the implicit scheme is at least 10 times faster. For viscous computations the gain of the implicit scheme is even greater, because unlike the implicit scheme, the explicit scheme does not always converge. The comparison of the reordered and nonreordered versions of the method shows that the method with reordering is about 30% faster. This is a typical gain in performance, which was obtained for all of the computed problems.

VI. Conclusions

The implicit LU-SGS method has been implemented to the three-dimensional hybrid unstructured grid cell-vertex finite volume computations. The method has shown its robustness for tetrahedral and hybrid unstructured grids. The implicit part of the method is fully vectorized and takes 70% of time required for explicit flux computations. The method is approximately 10 times faster (depending on the concrete problem) as compared to the explicit method with local time stepping. The proposed reordering algorithm is approximately 30% faster than the method without reordering. Extra storage of the proposed method is approximately 5% of the total memory requirements.

References

[1]Jameson, A., and Yoon, S., "Lower-Upper Implicit Schemes with Multiple Grids for the Euler Equations," *AIAA Journal*, Vol. 25, No. 7, 1987, pp. 929–935.

[2]Men'shov, I., and Nakamura, Y., "Implementation of the LU-SGS Method for an Arbitrary Finite Volume Discretization," *9th Japanese Symposium on CFD*, Chuo Univ., Tokyo, Japan, 1995, pp. 123,124.

[3]Soetrisno, M., Imlay, S. T., and Roberts, D. W., "A Zonal Implicit Procedure for Hybrid Structured–Unstructured Grids," AIAA Paper 94-0645, Jan. 1994.

[4]Soetrisno, M., Imlay, S. T., Roberts, D. W., and Taflin, D. E., "Development of a 3-D Zonal Implicit Procedure for Hybrid Structured–Unstructured Grids," AIAA Paper 96-0167, Jan. 1996.

[5]Venkatakrishnan, V., "On the Accuracy of Limiters and Convergence to Steady State Solutions," AIAA Paper 93-0880, Jan. 1993.

[6]Obayashi, S., and Guruswamy, G. P., "Convergence Acceleration of an Aeroelastic Navier–Stokes Solver," AIAA Paper 94-2268, June 1994.

[7]Sharov, D., and Nakahashi, K., "Hybrid Prismatic/Tetrahedral Grid Generation for Viscous Flow Applications," *AIAA Journal*, Vol. 36, No. 2, 1998, pp. 157–162 (AIAA Paper 96-2000).

J. Kallinderis
Associate Editor

Numerical Simulation of Two-Dimensional Transverse Gas Injection into Supersonic External Flows

R. Dhinagaran* and T. K. Bose†
Indian Institute of Technology, Madras 600 036, India

Introduction

THE flowfield resulting from the injection of a transverse gas jet into a supersonic crossflow finds many applications such as thrust vector control in rocket motors, reaction control of missiles, and fuel injection in supersonic combustors and in supersonic fluidics. A typical jet interaction flowfield is shown in Fig. 1a. The injected underexpanded jet acts as an obstacle in the inviscid region inducing a bow-shaped shock called the induced bow shock. The pressure rise due to the induced shock separates the boundary layer ahead of the jet causing, in general, a separation shock. The strength of the separation shock depends very much on the nature of the boundary layer, that is, laminar, turbulent, or transitional. Typical pressure distributions for these types of separation are shown in Fig. 1b. In the case of a laminar boundary layer, separation is provoked even at a small adverse pressure gradient because the shear stress, which balances the pressure gradient, in the laminar regime is minimum. Therefore, the pressure peak is also small. The value of peak pressure for transitional separation can vary from slightly greater than that for pure laminar to a value less than that for turbulent separation depending on the position of transition as is shown in Fig. 1b. The jet upon exiting from the slot expands rapidly until it attains pressure equilibrium with the freestream through a normal shock, often termed the Mach disk. Just downstream of the slot, the jet expands, resulting in a pressure drop below that of the undisturbed value. Farther downstream, the flow is compressed to move parallel to the plate through a recompression shock. Two counter-rotating vortices upstream and a recirculation zone downstream of the slot are observed. The present study is aimed at numerically simulating the experimental data of Spaid and Zukoski[1] (runs 10–13, 16, and 17) corresponding to turbulent and transitional separations for a wide range of secondary jet to freestream total pressure ratios ($0.187 < Po_s/Po_p < 4.306$).

Received Nov. 1, 1994; revision received Oct. 9, 1997; accepted for publication Dec. 4, 1997. Copyright © 1998 by the American Institute of Aeronautics and Astronautics, Inc. All rights reserved.

*Research Scholar, Department of Aerospace Engineering.

†Professor, Department of Aerospace Engineering. Associate Fellow AIAA.

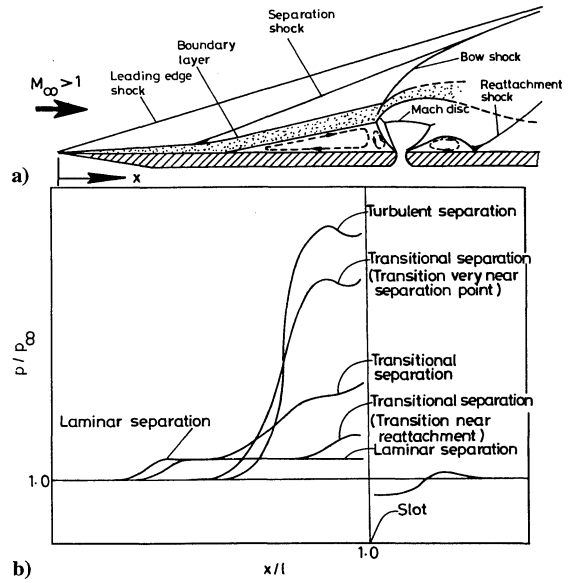

Fig. 1 Schematic of a) jet interaction flowfield and b) associated surface pressure distributions for different separation regimes.

Numerical Analysis

The unsteady compressible mass averaged Navier–Stokes equations in two dimensions in strong conservation form are taken as the governing equations. The molecular viscosity is evaluated from Sutherland's formula, and turbulent eddy viscosity is obtained from the two-layer isotropic turbulence model due to Baldwin and Lomax[2] (BL). The laminar and turbulent Prandtl numbers are taken as $Pr_l = 0.72$ and $Pr_t = 0.9$, respectively. A step transition is set at 6.35 cm from the plate leading edge for the turbulent separation case, concurrent with the experimental observations.[1] For transitional separation, transition is prescribed to start at the location where pressure starts rising in the upstream and to end at the slot location. In the absence of experimental data, this choice is reasonable because the flow turns in any case to become nearly turbulent at the slot due to the shear layers formed by injection. At the upstream computational boundary, located just ahead of the leading edge of the plate, and on the top boundary, which is located sufficiently far from the plate, all of the variables are held fixed at supersonic inflow conditions. At the exit all variables are linearly extrapolated from the interior. On the plate surface no-slip and adiabatic conditions are imposed. At the slot, all variables are held fixed at sonic conditions. For the turbulent separation cases in which Po_s/Po_p are large, upstream separation prevails for a large distance. The BL model is known to predict a sharp increase in the outer layer eddy viscosity in such cases near the separation shock. As a remedy, relaxation terms are introduced in the equilibrium model (BL model here) that account for the upstream turbulence history effects.[3] Two relaxation models are attempted in this study.

The first is the upstream relaxation (UPR) model, where

$$\varepsilon = \varepsilon_{eq} - (\varepsilon_{eq} - \varepsilon_0)\exp[-(x - x_0)/\lambda]$$

and the second is the point-by-point relaxation (PPR) model, where

$$\varepsilon^i = \varepsilon^i_{eq} - \left(\varepsilon^i_{eq} - \varepsilon^{i-1}\right)\exp\left(-\frac{x_i - x_{i-1}}{\lambda}\right)$$

where ε is the eddy viscosity after relaxation; ε_{eq} is the equilibrium eddy viscosity calculated from the BL model; ε_0 is the eddy viscosity at the point x_0, at which the upstream pressure starts rising; and λ is the relaxation length. The value of λ depends on the flow Mach number but a constant λ is found to yield reasonably accurate predictions for a wide range of flow parameters.[3] The PPR model avoids the specification of x_0 and instantly accounts for local upstream turbulence history. The distance from the plate leading edge to the centerline of the slot $l = 0.2286$ m, slot width $w = 0.2667$ mm, is taken according to the experimental conditions. The distance from the centerline of the slot to the exit boundary of the computational domain is prescribed as 0.1524 m. Effects of mesh spacing were tested for the representative case $Po_s/Po_p = 0.425$ in which a grid of 118×56 cells was found to give grid-independent results. Therefore, the computational domain is divided into 118×56 cells for all cases except for the case $Po_s/Po_p = 1.5788$, which has the largest upstream separation, where 168×56 cells are used. This is done to have a nearly uniform mesh spacing in the x direction for all cases. Grid in the y direction is stretched from the plate surface to the upstream computational domain using exponential functions. The law of the wall coordinate y^+ for the first mesh point has been maintained as <5 in all cases. The governing equations are integrated in time using the explicit, time-split, second-order-accurate, finite volume scheme of Hung and MacCormack.[4] The dissipation terms required for the stability of the calculations are similar to those of Harten and Zwas.[5] A Courant–Friedrichs–Lewy number of 0.7 produced stable results. About 15,000 time steps are required, in general, for convergence, corresponding to a three-order drop in density residual.

Results and Discussion

Representative computed Mach number contours and the velocity field for the turbulent separation case are shown in Fig. 2, illustrating the numerically captured flow features. The induced and separation shocks can be observed, along with the Mach disk. The recompression shock is also fairly visible. The two counter-rotating vortices upstream and a recirculation zone downstream of the slot are also predicted (Fig. 2b). Similar features also were observed in the transitional separation case (not shown).

Among the turbulent separation cases, agreement between computed and measured pressures is excellent in the upstream side of the slot for the cases with $Po_s/Po_p = 0.218$ and 0.426, whereas in the downstream side expansion is slightly underpredicted (Fig. 3a). The overall agreement is very good for these cases. For cases with higher Po_s/Po_p(= 0.805 and 1.579), the upstream pressure propagation is underpredicted and the peak pressure is overpredicted. This is due to the large values of turbulent eddy viscosity generated by the BL model in these cases. A similar phenomenon was observed by Hung[3] in the computation of supersonic compression ramp flows. These two cases have been computed again, incorporating relaxation terms in the BL model, the results of which are discussed later. For transitional separation cases, computed pressures agree with the measured values qualitatively. In the upstream region, near separation, pressure starts increasing gradually, as opposed to the sudden pressure

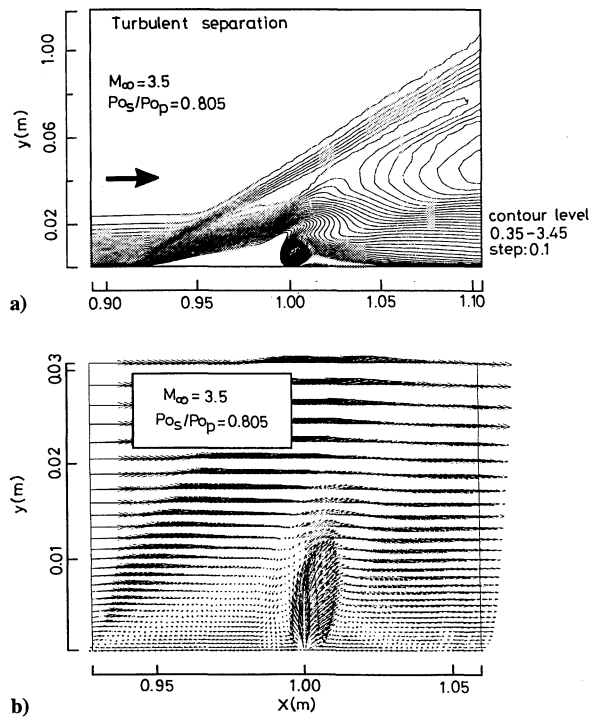

Fig. 2 Representative a) Mach number contour plot and b) velocity field.

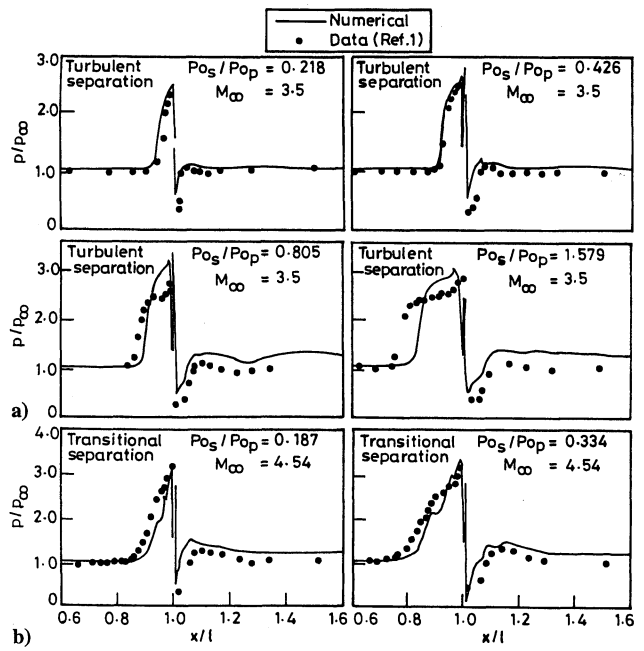

Fig. 3 Comparison of predicted and measured surface static pressures for a) turbulent and b) transitional separations.

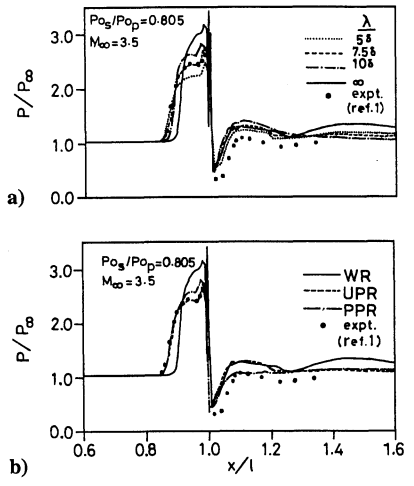

Fig. 4 Surface static pressure distributions depicting a) the effect of relaxation length and b) the performance of the two relaxation models.

rise found in the turbulent separation cases. Upstream pressures are underpredicted, whereas downstream pressures are overpredicted. However, the overall trend is very encouraging despite the crude transition model used.

In an attempt to extend the applicability of the BL model for jet interaction flows with large upstream separation, relaxation terms are incorporated in the present study. The values of x_0, the point at which upstream pressure starts increasing, are taken as 0.1886 m for $Po_s/Po_p = 0.805$ and 0.1715 m for $Po_s/Po_p = 1.579$ (from experiments). To apply the model, the relaxation length λ has to be determined first. Figure 4a shows the effect of λ on the surface pressure distribution. The case $\lambda = \infty$ corresponds to the equilibrium model, that is, without relaxation (WR). Decreasing λ increases the upstream pressure propagation and decreases the upstream pressure peak. The optimum λ for this case is found to be $7.5\delta_0$, where δ_0 is the boundary-layer thickness at x_0 (Fig. 4a). For the case with $Po_s/Po_p = 0.805$, both models predict the same upstream separation location (Fig. 4b). Though the PPR model overpredicts the upstream pressure peak slightly, it is excellent in the downstream pressure prediction. For the highest pressure ratio case ($Po_s/Po_p = 1.579$), the PPR model underpredicts the upstream pressure propagation although there is some improvement when compared to the equilibrium model (WR). The UPR model predicts the upstream pressure distribution well and, therefore, gives a better overall prediction. In general, significant improvement is observed in the predictions with the incorporation of relaxation terms.

Conclusions

Jet interaction flowfields with turbulent and transitional separation for a wide range of freestream to injectant total pressure ratios are simulated numerically. Calculations with the BL model show reasonably accurate results, in general, except for flows with large injectant-to-freestream-total-pressure ratios attended by large upstream separation, where it underpredicts the upstream separation and overpredicts the upstream peak pressure. With the inclusion of relaxation terms in the BL model, significant improvement in terms of better upstream pressure propagation and reduced peak pressure over those without relaxation are obtained. Of the two relaxation models used, the UPR model performs better. In the case of transitional separation, qualitative agreement is observed, despite the crude transition model employed.

References

[1]Spaid, F. W., and Zukoski, E. E., "A Study of the Interaction of Gaseous Jets from Transverse Slots with Supersonic External Flows," *AIAA Journal*, Vol. 6, No. 2, 1968, pp. 205–212.

[2]Baldwin, B., and Lomax, H., "Thin Layer Approximation and Algebraic Model for Separated Turbulent Flows," AIAA Paper 78-257, 1978.

[3]Hung, C. M., "Development of Relaxation Turbulence Models," NASA CR-2783, Dec. 1976.

[4]Hung, C. M., and MacCormack, R. W., "Numerical Solutions of Supersonic and Hypersonic Laminar Compression Corner Flows," *AIAA Journal*, Vol. 14, No. 4, 1976, pp. 475–481.

[5]Harten, A., and Zwas, G., "Switched Numerical Shumann Filters for Shock Calculations," *Journal of Engineering Mathematics*, Vol. 6, No. 2, 1972, pp. 207–216.

F. W. Chambers
Associate Editor

Mach Reflection Wave Configuration in Two-Dimensional Supersonic Jets of Overexpanded Nozzles

H. Li* and G. Ben-Dor†
Ben-Gurion University of the Negev, Beer-Sheva 84105, Israel

Introduction

A CONVERGING/DIVERGING nozzle is a device by which supersonic flows can be produced. Applications of such flows are supersonic wind tunnels, rocket nozzles, gas lasers, etc. An excellent and comprehensive discussion of the possible flows through such nozzles is given in Ref. 1. The ambient pressure P_∞ is the key parameter in determining the nature of the flow in the nozzle and the jet emanating from it. When the exit flow is supersonic, the exit plane pressure P_3 may be larger, equal, or smaller than P_∞. When $P_3 < P_\infty$, the nozzle is overexpanded and two oblique shock waves are formed at the lips of the nozzle (Fig. 1a). The interaction of these oblique shock waves results in either a regular or a Mach reflection (Fig. 1a). In overexpanded nozzles, an analytical solution exists only when the resulting wave configuration is a regular reflection. An analytical solution for situations in which the

Received Feb. 14, 1996; accepted for publication Nov. 29, 1997. Copyright © 1998 by the American Institute of Aeronautics and Astronautics, Inc. All rights reserved.

*Postdoctoral Fellow, Department of Mechanical Engineering.

†Professor, Dean of the Faculty of Engineering Sciences, Pearlstone Center for Aeronautical Engineering Studies, Department of Mechanical Engineering.